Pharmaceutical Research, Vol. 25, No. 3, March 2008 (© 2007)
DOI: 10.1007/s11095-007-9397-y

Research Paper

The Role of Permeability in Drug ADME/PK, Interactions and Toxicity—Presentation of a Permeability-Based Classification System (PCS) for Prediction of ADME/PK in Humans

Urban Fagerholm[1,2]

Received May 11, 2007; accepted June 26, 2007; published online August 21, 2007

Purpose. The objective was to establish *in vitro* passive permeability (P_e) vs *in vivo* fraction absorbed (f_a)-relationships for each passage through the human intestine, liver, renal tubuli and brain, and develop a P_e-based ADME/PK classification system (PCS).
Materials and Methods. P_e- and intestinal f_a-data were taken from an available data set. Hepatic f_a was calculated based on extraction ratios of the unbound fraction of drugs (with support from animal *in vivo* uptake data). Renal f_a (reabsorption) was estimated using renal pharmacokinetic data, and brain f_a was predicted using animal *in vitro* and *in vivo* brain P_e-data. Hepatic and intestinal f_a-data were used to predict bile excretion potential.
Results. Relationships were established, including predicted curves for bile excretion potential and minimum oral bioavailability, and a 4-Class PCS was developed: I (very high P_e; elimination mainly by metabolism); II (high P_e) and III (intermediate P_e and incomplete f_a); IV (low P_e and f_a). The system enables assessment of potential *drug–drug* transport interactions, and drug and metabolite organ *trapping*.
Conclusions. The PCS and high quality P_e-data (with and without active transport) are believed to be useful for predictions and understanding of ADME/PK, elimination routes, and potential interactions and organ *trapping*/toxicity in humans.

KEY WORDS: absorption; classification system; *drug–drug* transport interactions; permeability; prediction.

This paper includes personal opinions of the author, which do not necessarily represent the views or policies of AstraZeneca.

[1] Clinical Pharmacology, AstraZeneca R&D Södertälje, S-151 85, Södertälje, Sweden.
[2] To whom correspondence should be addressed. (e-mail: urban.fagerholm@astrazeneca.com)

ABBREVIATIONS: ADME/PK, AbsorptionDistributionMetabolismExcretion/Pharmacokinetics; a.s., active secretion; BBB, blood–brain barrier; BCS, Biopharmaceutics Classification System; BDDCS, Biopharmaceutics Drug Disposition Classification System; BUI, brain uptake index; C_{bl}/C_{pl}, blood-to-plasma concentration ratio; CL, clearance; CL_H, hepatic CL; CL_{int}, intrinsic CL; $CL_{int,secr}$, renal tubular secretion CL_{int}; CL_R, renal CL; E_H, hepatic extraction ratio; EHC, enterohepatic circulation; $E_{u,H}$, E_H for unbound drug; $E_{max,bile}$, maximum bile excretion potential; $E_{u,R}$, renal extraction ratio for unbound drug; $E_{1st\text{-}pass}$, first-pass extraction ratio; F, oral bioavailability; f_a, fraction absorbed; $f_{a,B}$, brain f_a; $f_{a,H}$, hepatic f_a; $f_{a,I}$, intestinal f_a; f_e, fraction of intravenous dose excreted unchanged in urine; F_{min}, minimum F; f_{ra}, fraction reabsorbed; $f_{ra,bile}$, fraction reabsorbed from the intestines following bile excretion; $f_{ra,R}$, fraction reabsorbed in the renal tubuli; f_u, unbound fraction; $f_{u,bl}$, f_u in blood; $f_{u,pl}$, f_u in plasma; GFR, glomerular filtration rate; GI, gastrointestinal; MDCK, Madin–Darby canine kidney cells; MW, molecular weight; P_e, permeability; PCS, P_e-based Classification System; P_eS, uptake CL (permeability–surface area product); P_{e50}, P_e corresponding to a f_a (or f_{ra}) of 0.50; PSA, polar surface area; Q, blood flow rate; Q_B, brain Q; Q_H, hepatic Q; Q_R, renal Q; S, surface area; S_B, brain S; TT, transit time; $t_{1/2}$, half-life; λ, slope factor.

INTRODUCTION

Permeability (P_e) is one of the main determinants for drug absorption, distribution, metabolism, excretion/pharmacokinetics (ADME/PK), and drug and metabolite tissue exposures. An understanding of the role of P_e in various organs is therefore crucial for predictions of ADME/PK, drug–drug-interactions, and drug and metabolite toxicity. The relationship between P_e and extent of drug uptake from the gastrointestinal (GI) tract in man has been well studied and established, but for many other important organs in drug ADME/PK, including the liver, kidneys and the brain, such relationships are not available or poorly investigated. An apparent reason is the lack of organ uptake data in humans. Thus, there is a requirement for a better knowledge and understanding of P_e and uptake capacities in these organs.

The organ uptake of substances with a P_e at and near the steepest part of the P_e *vs* fraction absorbed (f_a) relationships is potentially more sensitive to involvement of and changes in P_e (such as results of saturated, inhibited and induced active transport, or changes in pH) than of compounds with high passive P_e. An establishment of P_e *vs* f_a for different organs involved in drug absorption and disposition could therefore be of great value for predicting and understanding potential drug–drug interactions, saturation, and cellular *trapping* of drugs and metabolites.

0724-8741/08/0300-0625/0 © 2007 Springer Science + Business Media, LLC

P_e is the rate (commonly expressed as 10^{-6} cm/s) at which a molecule passes through endothelial and epithelial cells. It is measured either as a disappearance from the donor side (such as in liver and intestinal perfusion studies) or an appearance on the receiver side (such as in *in vitro* P_e-studies and *in vivo* brain microdialysis studies). The interplay between the P_e, surface area (S), pH and residence time in the absorptive region, blood component binding capacity, and the molecular characteristics, determine the extent and fraction of absorption during each passage through tissues and organs. Compounds with P_e-values greater than zero across cells will be absorbed to some extent, and if time permits, the uptake will eventually be complete or equilibrium will be reached.

The transepithelial and -endothelial passage of drugs and metabolites occurs by passive diffusion, and in quite many cases, active transport (uptake and/or efflux) is also involved. Membranes on opposite sides of cells are often characterised by different composition and transport proteins (see below). Permeation across the cells (transcellular route) is generally believed to be the main route. It has been debated whether or not drug transport via the paracellular (between cells) route is of importance. According to studies in the human intestine *in vivo* it appears that paracellular uptake of molecules with a molecular weight (MW)>200 g/mole is negligible (1). This is consistent with the relative small area of the paracellular space (~1/10,000 in the small intestine), and probably even smaller in the blood–brain barrier (BBB) (1), and a paracellular diameter (~16 and ~6 Å in the human small and large intestines, respectively) that is of similar size as spaces between the cell membrane phospholipids and cholesterol chains (~4 to ~10 Å) (2). Diffusion across a comparably unstirred layer of fluid adjacent to endothelia and epithelia, such as the mucus layer in the intestines and space of Disse in the liver, do not seem to have a significant influence on tissue uptake *in vivo* in humans (3,4). It could, however, influence *in vitro* P_e-measurements. Nearly complete liver extraction (>0.98) for many compounds indicates that the diffusion in the liver is no major limit *in vivo* (4).

Wu and Benet (5) developed a modified version of the Biopharmaceutics Classification System (BCS), the Biopharmaceutics Drug Disposition Classification System (BDDCS), suggested to be useful in predicting the overall drug disposition, including elimination routes and impact of active transport in drug absorption. In the BDDCS, the major route of elimination serves as the P_e-criteria. According to this system, the predominant elimination route for Class I (extensive metabolism—high solubility) and II (extensive metabolism—low solubility)-drug products is hepatic metabolism, while renal and/or biliary elimination of unchanged drug is the major route for III (poor metabolism—high solubility) and IV (poor metabolism—low solubility)-drug products. It is proposed that transporter effects for oral absorption are or could be important for Class II, III and IV-drug products.

Limitations with the BCS include a very strict solubility/dissolution limit (and thereby incorrect classification of many *in vivo* Class I products into Class II), a generous P_e-limit (≥14-times higher rate constant limit for dissolution than for permeation), strictness for drugs with long half-life ($t_{1/2}$), poor performance of human *in vivo*, *in vitro*, and in silico P_e-methods to classify the P_e for moderately to highly permeable substances, and underprediction potential of *in vivo* dissolution (6). In contrast to the number of substances in BCS Class II [about 1/3; (5)] it has only been possible to clearly find/define a few highly permeable drug products with solubility/dissolution-limited GI uptake in humans (out of more than 70 drug products) (6). These are danazol, and griseofulvin and atovaquone in the fasted state. Ways to improve the BCS have recently been suggested (6). The BCS and BDDCS share the strictness on solubility/dissolution. Further limitations with the BDDCS are the apparent lack of human *in vivo* bile excretion data (to verify bile excretion of Class III and IV-compounds), the potential for extensive gut-wall and hepatic extraction of compounds with limited P_e, and the possibility that eliminating organs show very different P_e and uptake capacities (e.g. low passive P_e in the renal tubuli and low passive+high active P_e in the liver). Figure 1 demonstrates the relationship between P_e-class [high; BCS Class I, low; BCS Class III, compounds were classified as being highly permeable if the intestinal f_a≥0.9 or when the P_e corresponds to a f_a≥0.9, absorption data were taken from Willmann *et al.* (7)] and three measurements of the importance of metabolism: 1-f_e, E_H and $E_{1st\text{-}pass}$ ($=1-F/f_a$). The f_e, E_H, $E_{1st\text{-}pass}$ and F are the fraction excreted in urine following intravenous dosing, hepatic extraction ratio, first-pass extraction ratio and oral bioavailability [data collected from Goodman Gilman (8)], respectively. The median and average estimates for highly permeable compounds are greater than those with low P_e, which is consistent with the basis for the BDDCS. There are, however, many low P_e-compounds with comparably high extent and degree of metabolism, and high P_e-drugs with minor metabolism. Thus, the BDDCS does not appear to be sufficiently robust for a good/poor solubility and extensive/poor metabolism classification. As shown and discussed below, the BDDCS (just like the BCS) appears to have a too low P_e-limit.

One objective was to try to establish relationships for passive *in vitro* P_e vs *in vivo* f_a for each passage through the human liver (including bile excretion), renal tubuli (reabsorption) and brain, and use these for development of a P_e-based ADME/PK classification system (PCS). A passive P_e-model was chosen in order to avoid potential influences of active transport. Except for intestinal f_a, human in vivo f_a-data for

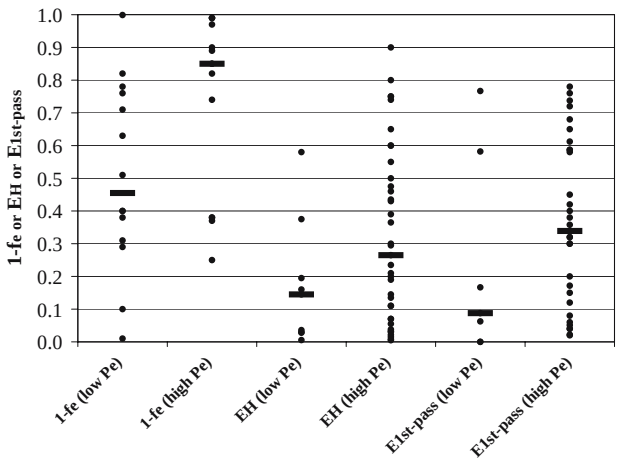

Fig. 1. The degree and extent of metabolism ($1-f_e$, E_H and $E_{1st\text{-}pass}$) for compounds with low and high P_e (according to the BCS and BDDCS) *in vivo* in humans. The number of observations (*filled circles*) per group is 9 to 27. The *lines* represent median values.

the liver, renal tubuli and brain are lacking. An aim was therefore to find possible ways to estimate and predict such data. Other aims were to evaluate the role of P_e in renal tubular secretion and accumulation, oral F, drug–drug interactions and hepatocyte *trapping* of metabolites.

MATERIALS AND METHODS

Equation 1 was used for establishing relationships between *in vitro* passive P_e and *in vivo* f_a for each passage through the human intestines ($f_{a,I}$), liver ($f_{a,H}$), renal tubuli ($f_{ra,R}$) and brain ($f_{a,B}$).

$$f_a = P_{e50}^{\lambda} \Big/ \left(P_{e50}^{\lambda} + P_e^{\lambda}\right) \tag{1}$$

P_{e50} is the P_e corresponding to a f_a (or f_{ra}) of 0.50 and λ is a shape factor. P_e-data used in this evaluation were taken from an extensive artificial membrane *in vitro* P_e-data set (n=126; including a large amount of registered drugs; obtained at pH 7.4) produced by Willmann *et al.* (7). The *in vitro* P_e was estimated from membrane affinities (defined as equilibrium partition coefficients between immobilized lipid bilayers and water). The $f_{a,I}$-data (n=126) were also taken from Willmann *et al.* (7).

No human hepatic P_e-, P_eS- or f_a-data are available (at least not to my knowledge). In order to find a possible relationship between P_e and $f_{a,H}$ in humans, the unbound hepatic extraction ratio ($E_{u,H}$; maximum $E_{u,H}$ is a surrogate for the maximum $f_{a,H}$) for several drugs (n=43) were estimated using Eq. 2:

$$E_{u,H} = CL_{int} / (CL_{int} + Q_H) \tag{2}$$

Data were calculated based on unbound fraction (f_u) in blood ($f_{u,bl}$), intrinsic CL (CL_{int}) and hepatic CL (CL_H)-data obtained from Obach (9) and Riley *et al.* (10). Q_H is the hepatic blood flow. This approach works under the assumption that the data set contains at least some compounds with apparent P_e-limited hepatic extraction of the unbound fraction. For such substances the $f_{a,H}$ equals the $E_{u,H}$. The rat hepatic $f_{a,H}$-data for unbound enalaprilat (P_e-limited hepatic metabolism; see below) were included in the analysis. The inclusion of this rat value was based on lack of human $E_{u,H}$-data for low P_e-compounds, and species similarities in membrane composition and passive P_e (11,12), species similarities in hepatic uptake of unbound acetylsalicylic acid (see Hepatic Uptake below), and allometric relationship for liver weight and Q_H (13,14).

The relationships between passive P_e *vs* $f_{a,I}$ and passive P_e *vs* $f_{a,H}$ can be used to predict the relationship between P_e and maximum bile excretion potential ($E_{max,bile}$) (Eq. 3).

$$\begin{aligned} E_{max,bile} = f_{a,H} \times \big[&(1 - f_{a,H}) + (f_{a,H} \times f_{a,I} \times (1 - f_{a,I})) \\ &+ (f_{a,H}^2 \times f_{a,I}^2 \times (1 - f_{a,I})) + (f_{a,H}^{\infty} \times f_{a,I}^{\infty} \times (1 - f_{a,I}))\big] \end{aligned} \tag{3}$$

The intestinal reabsorption (following bile excretion) and enterohepatic circulation (EHC) are considered. The newly developed Eq. 3 is based on the fractional bile excretion (with consequent feces excretion) for each circulation (until infinity), and the total $E_{max,bile}$ is the cumulative fraction of absorbed intact drug that is excreted in bile/feces. A too low P_e (low $f_{a,H}$ and $f_{a,I}$) implies that a minor fraction will be absorbed into the liver, and then secreted with bile, and a too high P_e (high $f_{a,H}$ and $f_{a,I}$) implies that the fraction excreted into the small intestine will be completely reabsorbed (and bile excretion will become a part of distribution and not elimination). A high passive P_e also increases the potential for a compound to be redistributed back to blood, and thereby, to escape transport (active secretion) into bile. An intermediate P_e is therefore expected to give the highest fraction of unchanged drug excreted with feces via the bile. Another prerequisite for extensive bile excretion to occur is that the hepatic metabolism is not too high (metabolism will then be the main route of elimination). The $E_{max,bile}$-approach assumes negligible transport from hepatocytes back to blood, continuous bile excretion, and negligible metabolism within hepatocytes. Hepatic metabolic CL_{int}-data could however be added when predicting the bile extraction ratio. The likelihood for passive transport into hepatocytes and then further into bile and small intestine appears small, and the bile secretion pattern in humans is irregular (see Bile Excretion Potential below). In order to visualize the role of P_e for bile excretion potential simulations were performed. Liver and intestinal P_e-data were set at various levels: passive transport in the absorptive directions (no active transport or passive efflux); complete uptake into bile and passive intestinal reabsorption; complete uptake into bile and passive intestinal reabsorption with 5-fold efflux ratio. The maximum intestinal fraction reabsorbed following bile excretion ($f_{ra,bile}$) was estimated based on passive uptake with a 5-fold efflux ratio.

The relationships between passive P_e *vs* $f_{a,I}$ and passive P_e *vs* $f_{a,H}$ can also be used to predict the impact of P_e on minimum oral bioavailability (F_{min}). If assuming passive transport, no solubility limitations [this is seldom a limitation for the extent of GI absorption (6)] and negligible gut-wall extraction, the F_{min} can be estimated using Eq. 4:

$$F_{min} = f_{a,I} \times (1 - f_{a,H}) \tag{4}$$

Relationships between P_e and observed F and $f_{a,I}$ and predicted F_{min} and $f_{a,I}$ were compared. F-data (n=33) were collected from Goodman Gilman (8).

In order to evaluate the tubular reabsorption capacity, renal CL (CL_R), f_e and f_u-data for renally excreted compounds were collected [from Goodman Gilman (8)] and analysed. Compounds were divided into two classes: those with apparent tubular reabsorption and apparent negligible active secretion, and those with apparent active secretion. $F_{ra,R}$-data for 9 compounds of the former class, and $1-E_{u,R}$ data for 13 substances of the latter class were estimated using Equations 5 and 6 (based on standard renal excretion equations), respectively. $E_{u,R}$ is the renal extraction ratio for unbound drug. The upper limit for $1-E_{u,R}$ is used as a surrogate measurement of the upper $f_{ra,R}$-limit (where passive tubular reabsorption capacity is sufficiently effective to reabsorb efficiently secreted compounds).

$$f_{ra,R} = (GFR \times f_{u,pl} - CL_R) / (GFR \times f_{u,pl}) \tag{5}$$

$$1 - E_{u,R} = 1 - ((CL_{int,secr} + GFR) / (CL_{int,secr} + Q_R + GFR)) \tag{6}$$

GFR, Q_R, $f_{u,pl}$ and $CL_{int,secr}$ are the glomerular filtration rate (125 ml/min), renal blood flow rate (Q_R=1,200 ml/min), f_u in

plasma and intrinsic tubular secretion, respectively (15,16). The $CL_{int,secr}$ was estimated using *in vivo* CL_R, f_u and Q_R-data. The relationships between passive P_e and CL_R (n=20) and passive P_e and f_e (n=23) were also investigated.

In order to make an approximation of human *in vivo* $f_{a,B}$ for unbound drug molecules (assuming no redistribution back to blood), relationships between log *in vitro* BBB P_e [taken from Lundquist et al. (17)] and log *in vivo* rat BBB P_e [taken from Lundquist et al. (17)], and artifical membrane *in vitro* P_e and *in vitro* BBB P_e, were used together with human brain S (S_B)- and Q (Q_B)-data and the well-stirred model (Eq. 7).

$$f_{a,B} = (P_e \times S_B)/(Q_B + P_e \times S_B) \quad (7)$$

It was assumed that humans and rats have similar *in vivo* BBB P_e. The S_B and Q_B were set to ~20 m^2 (18) and 610 ml/min (14), respectively.

In addition, the relationship between P_e and $f_{u,bl}$ was investigated. The $f_{u,pl}$- and blood/plasma concentration ratio (C_{bl}/C_{pl})-data used for the estimation of $f_{u,bl}$ ($f_{u,bl}$=((1−hematocrit)×$f_{u,pl}$)/(C_{bl}/C_{pl})) were collected from Shibata *et al.* (4), Obach (9), Sawada *et al.* (19,20), Poulin and Theil (21) and Fagerholm and Björnsson (22).

The P_e *vs* f_a-relationships in the different organs/tissues were the basis for the development of a P_e-based ADME/PK classification system (PCS) with four classes (I–IV), and for evaluating potential drug–drug interactions and organ accumulation, *trapping* and toxicity of drugs and metabolites.

RESULTS

Based on PK data, including CL_R, f_e, $E_{u,H}$ and $E_{u,R}$, and animal *in vitro* and *in vivo* brain P_e data (see equations) it was possible to estimate/predict the $f_{a,H}$, $f_{ra,R}$ and $f_{a,B}$ *in vivo* in humans quite well. *In vitro* passive P_e *vs in vivo* f_a- and f_{ra}-relationships were established for the studied organs, including predicted curves for $E_{max,bile}$ and F_{min}. P_{e50}- and λ-estimates for each of the studied organs are presented in Table I. The liver, followed by the intestines, has the highest absorptive capacity (low P_{e50}) for each passage, whereas the brain appears to have the lowest capacity (highest P_{e50}). The liver, followed by the brain, also has the highest % f_a per second (no renal data available due to lack of TT and S data). The brain has the highest % f_a per minute per S. Active transport seems to be common, and this adds some uncertainty to the established P_e *vs* f_a relationships. The impact of active transport seems to be pronounced in the kidneys. PCS with 4 Classes was developed: I (very high P_e; expected to be eliminated mainly by metabolism); II (high P_e) and III (intermediate P_e and incomplete f_a); IV (low P_e and f_a; lowest metabolism and highest renal excretion potentials). The Classes and characteristics of the PCS, and reference compounds are presented in Table II. Figures 1, 2, 3, 5, 6, 7 and 10 demonstrate the relationships between *in vitro* passive P_e and the uptake from various organs. Figures 4 and 5 show the relationships between *in vitro* passive P_e and $E_{max,bile}$ and F (including F_{min}), respectively. The impact of passive P_e on renal elimination is shown in Figs. 8, 9 and 11. Figure 12 shows the relationship between *in vitro* passive P_e and $f_{u,bl}$.

DISCUSSION

Intestinal Absorption and First-Pass Extraction

The P_{e50} and λ for this data set are approximated to 0.66×10^{-6} cm/s and 1.6, respectively (Table I). The most pronounced deviations from the apparent sigmoidal logarithmic P_e-linear $f_{a,I}$ relationship are compounds with active uptake and efflux.

In vitro P_e-data were obtained at a slightly higher pH (7.4) than in the upper small intestine. The average fasted state pH in the human duodenum, jejunum and ileum has been reported to be 6.5, 6.6 and 7.4, respectively (23,24). Other reported pH-values for the proximal small intestine in the fasted state are 5.1±0.6, 6.6±0.5 and 7.1±0.6 (25). The pH in the fluid adjacent to the enterocytes *in vivo* is one unit lower than in the lumen. The pH drops below 6 at the entry into the colon, and is then raised to ~7 in the distal parts (26). Some of deviations from the P_e *vs* $f_{a,I}$-relationship could therefore have been due to differences in degree of ionization (for weak acids and bases).

Enalaprilat ($f_{a,I}$=0.10), amiloride, ($f_{a,I}$=0.50), atenolol ($f_{a,I}$=0.54), etoposide ($f_{a,I}$=0.50), betaxolol ($f_{a,I}$=0.90), chloramphenicol ($f_{a,I}$=0.90), cimetidine ($f_{a,I}$=0.85), clonidine ($f_{a,I}$=0.95), diltiazem ($f_{a,I}$=0.92), flunitrazepam ($f_{a,I}$=0.90), hydrocortisone ($f_{a,I}$=0.90), methylprednisolon ($f_{a,I}$=0.82), phenytoin ($f_{a,I}$=0.90) and pindolol ($f_{a,I}$=0.92) are suitable reference compounds for low, intermediate and high intesti-

Table I. Physiological Parameters and P_{e50}-, λ- and f_a-estimates for the Human Intestines, Liver, Renal Tubuli and Brain

	Intestines	Liver	Renal tubuli	Brain
Transit time (s)	30,000[a]	31	n.i.	5
Surface area (m^2)	70	180	n.i.	20
P_{e50} ($\times10^{-6}$ cm/s)	0.66	0.33	1.4/12[b]	24
λ	1	1.6	3.3/5[b]	2/0.7[c]
f_a at P_e=1×10^{-6} cm/s (%)	66	75	25/0	3
-"- (average % per s)	0.002	2.4	–/–	0.6
-"- (average % per min per m^2)	0.002	0.8	–/–	1.8

See text for references
n.i. No information available
[a] Based on an effective intestinal transit time of 8.4 h (81,82)
[b] Compounds with no apparent active secretion/efficient active secretion
[c] At low P_e

Table II. The Classes and Characteristics of the PCS, and Reference Compounds

Class	Characteristics	Reference compounds
I	Very high P_e; $>20\times10^{-6}$ cm/s	$P_e\approx20\times10^{-6}$ cm/s for amlodipine, haloperidol and nifedipine
	Complete passive hepatic and intestinal absorption	
	Complete passive tubular reabsorption and low CL_R regardless of active secretion	
	Low bile excretion potential	
	In general, $CL_H>>CL_R$ and CL_{bile} (especially when predicted *in vivo* metabolic $CL_{int}>300$ ml/min)	
	Very rapid and extensive passive brain uptake	
	Brain uptake potentially sensitive to active transport and related interactions	
II	High P_e; $2.5<P_e<20\times10^{-6}$ cm/s	$P_e\approx20\times10^{-6}$ cm/s for amlodipine, haloperidol and nifedipine
	Complete or near complete passive hepatic and intestinal absorption	$P_e\approx2.5\times10^{-6}$ cm/s for cimetidine, caffeine, probenecid and warfarin
	Complete or near complete passive tubular reabsorption, and low CL_R when no active renal secretion	
	Bile excretion potential if efficient active bile excretion and intestinal efflux, and low metabolic CL_{int}	
	Rapid and extensive passive brain uptake	
III	Intermediate P_e; $0.25<P_e<2.5\times10^{-6}$ cm/s	$P_e\approx2.5\times10^{-6}$ cm/s for cimetidine, caffeine, probenecid and warfarin
	Intermediate passive hepatic and intestinal absorption	$P_e\approx0.25\times10^{-6}$ cm/s for nadolol and sulpiride
	Poor to extensive CL_R	
	Bile excretion potential if efficient active bile excretion and intestinal efflux, and low metabolic CL_{int}	
	At least ~0.05–0.2 oral F if passive uptake, negligible E_{GW} and good GI solubility	
	Moderately rapid passive brain uptake	
IV	Low P_e; $<0.25\times10^{-6}$ cm/s	$P_e\approx0.25\times10^{-6}$ cm/s for nadolol and sulpiride
	Incomplete passive hepatic and intestinal absorption Oral F mainly determined by intestinal f_a	
	No passive tubular reabsorption	
	Low blood binding potential	
	Maximum f_e-potential	
	Slow passive brain uptake	

nal P_e. Metoprolol ($f_{a,I}$=0.98) can serve as a reference compound of limit for complete intestinal absorption.

The gut-wall/hepatic CL ratio for the highly permeable and moderately extracted CYP3A4-substrate midazolam is only 1/35 (27), which indicates that the systemic gut-wall CL generally can be neglected when predicting the total CL. First-pass gut-wall extraction could, however, be of importance, especially for substrates of CYP3A4 (including midazolam) and conjugating enzymes (28,29). Colonocytes have a different expression and generally lower activities of drug metabolizing enzymes than enterocytes (except for conjugating enzymes), and they are, therefore, expected to contribute less to drug metabolism (30–32). In comparison, they are also less permeable to compounds with low and intermediate P_e (33). Thus, a fraction of oral doses of compounds (mainly substrates of CYP3A4 and conjugating enzymes) not completely absorbed from the small intestine (those with low and intermediate P_e) could escape some of the first-pass gut-wall extraction.

The total effective (not similar to the anatomic) apical S of the human small intestine is approximated to 70 m^2 (7), and the transit time (TT) in the small and large intestines are reported to be 3±1 and 36 (range 1 to >60) h, respectively (35). The incomplete uptake of many compounds despite the

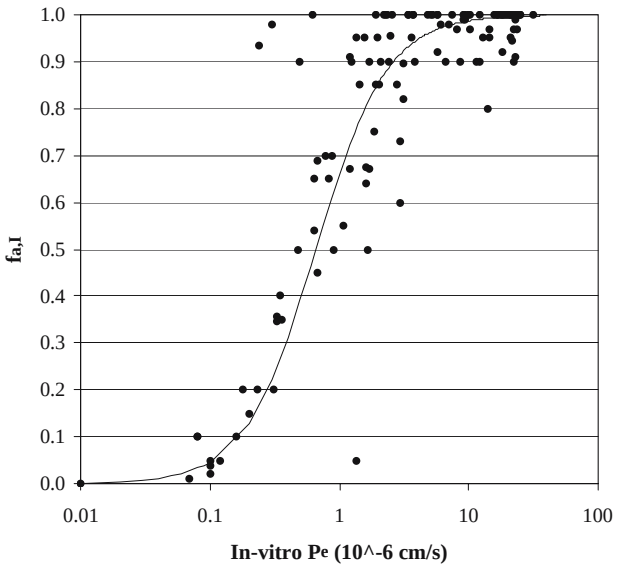

Fig. 2. The relationship between *in vitro* artificial membrane P_e and *in vivo* $f_{a,I}$ in humans (n=126). The *filled circles* are observations and the line is the fit.

comparably large S and long time for absorption shows the comparably low P_e of intestinal cells.

Hepatic Uptake

Hepatocytes, which are mainly responsible for the hepatic drug metabolism are highly permeable compared with many other cells (35). P_e-estimates for water, urea, erythritol and mannitol in isolated rat hepatocytes are higher than those obtained in the perfused rat and human small intestine (water, urea), red blood cells (water, urea, erythritol, mannitol), lung cells (water), BBB cells (mannitol, urea) and Caco-2 (colonic carcinoma) cells (mannitol, urea)

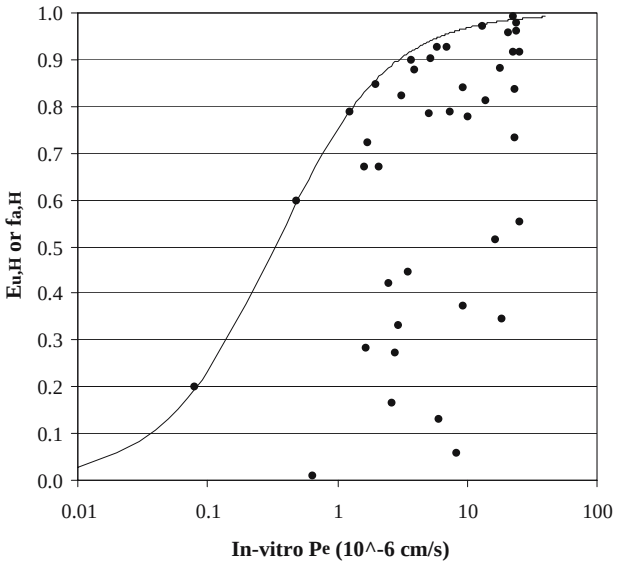

Fig. 3. The relationship between *in vitro* artificial membrane P_e and *in vivo* $E_{u,H}$ or $f_{a,H}$ in humans (n=43). The *filled circles* are the P_e vs $E_{u,H}$-observations and the *line* is the P_e *vs* $f_{a,H}$-fit.

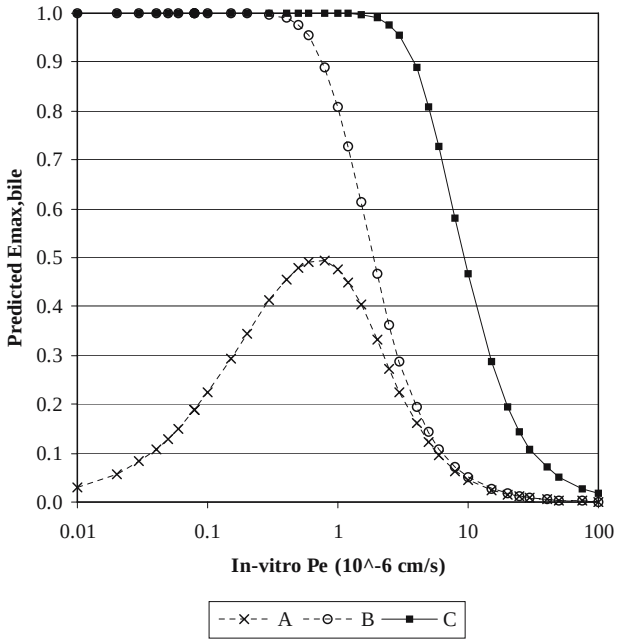

Fig. 4. The predicted relationships between *in vitro* artificial membrane P_e and *in vivo* $E_{max,bile}$ in humans for different hypothetical compounds. Liver and intestinal P_e-data were set at various levels: **a** passive transport in the absorptive directions (no active transport or passive efflux); **b** complete uptake into bile and passive intestinal reabsorption; **c** complete uptake into bile and passive intestinal reabsorption with 5-fold efflux ratio.

(1,17,35). The liver also has a comparably large *S*. The total sinusoidal *S* of hepatocytes in the human liver can be approximated (to 180 m^2) by multiplying the sinusoidal *S* ($\sim 0.1 \times 10^{12}$ μm^2/g liver) and liver weight (~1,800 g) (15,36). The hepatic TT for blood and an unbound non-absorbable

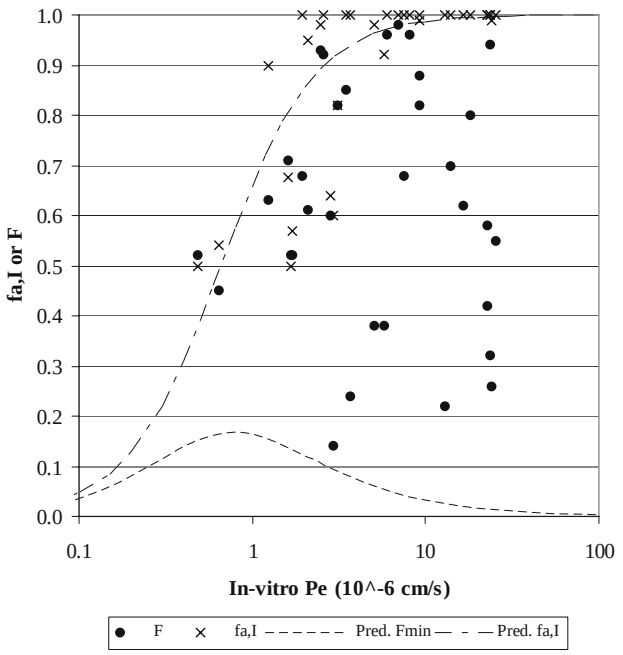

Fig. 5. The relationship between observed *in vitro* artificial membrane P_e and *in vivo* $f_{a,I}$ (n=33; *crosses*) and *F* (n=33; *filled circles*) and predicted $f_{a,I}$ and F_{min} (*dotted lines*) in humans.

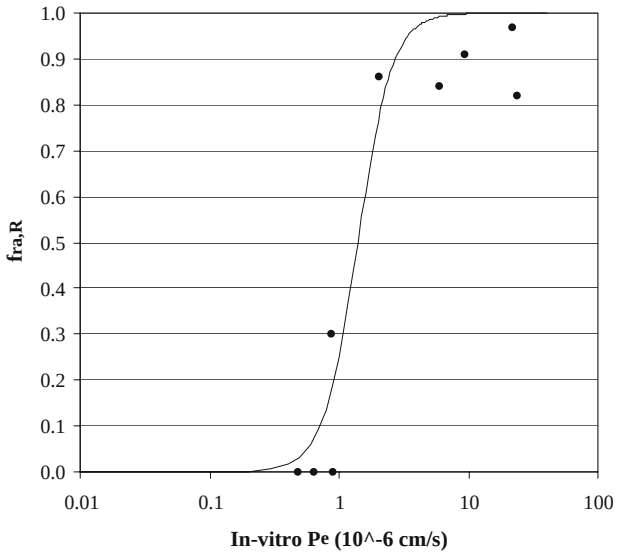

Fig. 6. The relationship between *in vitro* artificial membrane P_e and *in vivo* renal tubular $f_{ra,R}$ for compounds with no apparent active secretion in humans (n=9). The *filled circles* are the observations and the line is the fit.

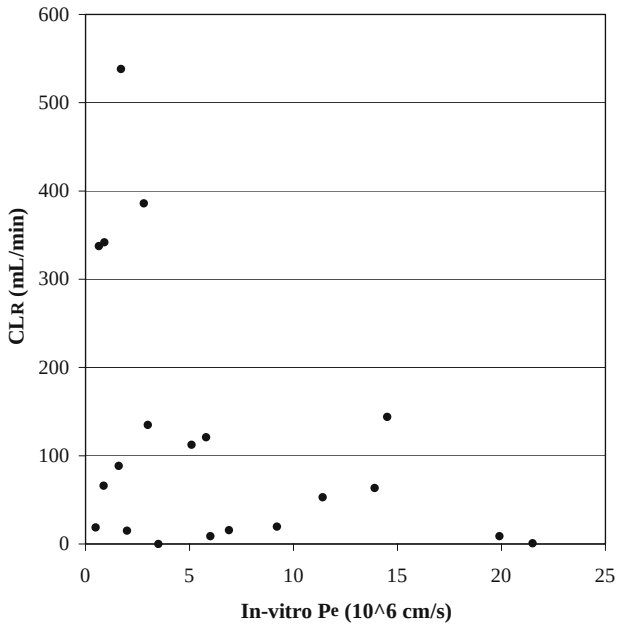

Fig. 8. The relationship between *in vitro* artificial membrane P_e and *in vivo* CL_R in humans (n=20).

compound are approximated to 20 and 31 s, respectively. These TT-estimates were calculated based on liver blood volume (0.5 l), Q_H (1.5 l/min), and 54% longer TT for unbound compared to blood cell-bound compounds (rat data) (14,15,37).

Rat *in situ* perfusion studies have shown that the hepatic P_eS is rate-limiting for the CL_H of enalaprilat (*in vitro* passive P_e=0.08×10^{-6} cm/s) (38). The influx P_eS of unbound enalaprilat in the rat liver was estimated to 0.35 ml/min/g liver, which is 25% of the Q_H and corresponds to a $f_{a,H}$ of 0.20 (38). The $f_{a,H}$ of unbound acetylsalicylic acid (*in vitro* passive P_e=1.94×10^{-6} cm/s) in rats, dogs and sheep has been estimated to 0.6 to 0.8 (39), which indicates similarities in hepatic uptake among species. The P_eS of unbound acetylsalicylic acid in the perfused rat liver is six to seven times higher than for free enalaprilat, and 50% higher than the Q_H (38,39).

Figure 3 shows that a relationship between P_e and maximum $E_{u,H}$ (~$f_{a,H}$) could be established. The P_{e50} and λ for this data set are approximated to 0.33×10^{-6} cm/s and 1.0,

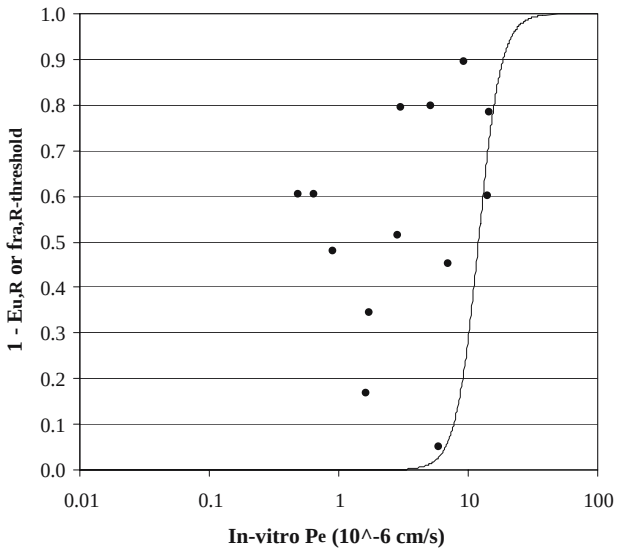

Fig. 7. The relationship between *in vitro* artificial membrane P_e and *in vivo* $1-E_{u,R}$ (or $f_{ra,R}$-threshold) for compounds with apparent active secretion in humans (n=13). The *filled circles* are the P_e *vs* $1-E_{u,R}$-observations and the line is the P_e *vs* $f_{ra,R}$-threshold fit.

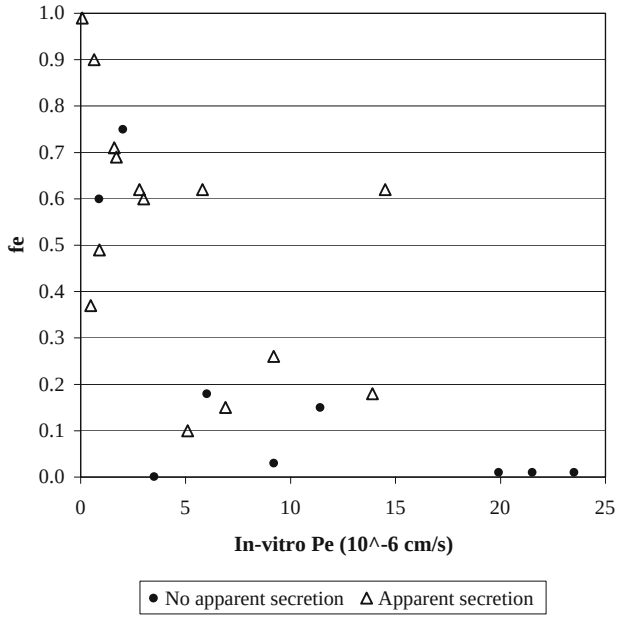

Fig. 9. The relationship between *in vitro* artificial membrane P_e and *in vivo* f_e in humans (n=23).

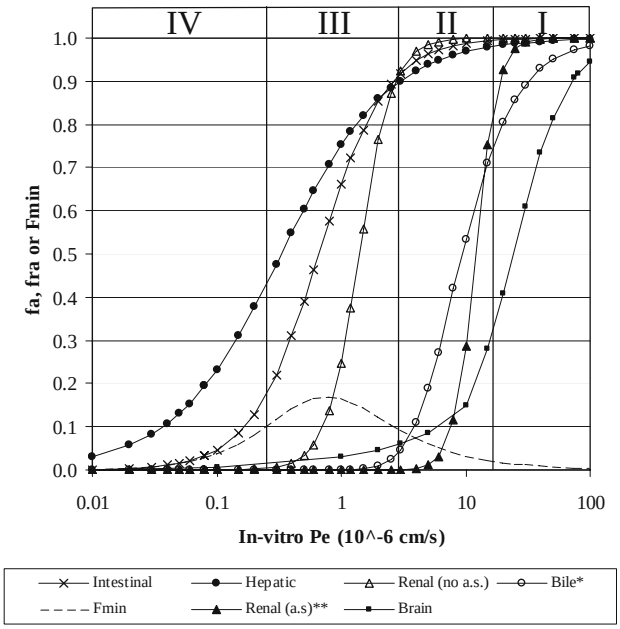

Fig. 10. The PCS and its classes (I–IV), and predicted relationships between *in vitro* artificial membrane P_e and *in vivo* f_a or f_{ra} for each passage in different organs (intestines, liver, brain, renal tubuli and bile) and F_{min}. *a.s* Active secretion. *Limit for intestinal reabsorption and bile excretion. The $f_{ra,bile}$ was calculated assuming a 5-fold intestinal efflux ratio. **Limit for tubular reabsorption and renal excretion.

respectively (Table I). The figure indicates that permeation is or probably is rate-limiting for the hepatic extraction of compounds with both intermediate and comparably high P_e. Enalaprilat ($f_{a,H}$ in the rat=0.20; *in vitro* passive P_e=0.08×10^{-6} cm/s), zidovudine ($E_{u,H}$=0.79; *in vitro* passive

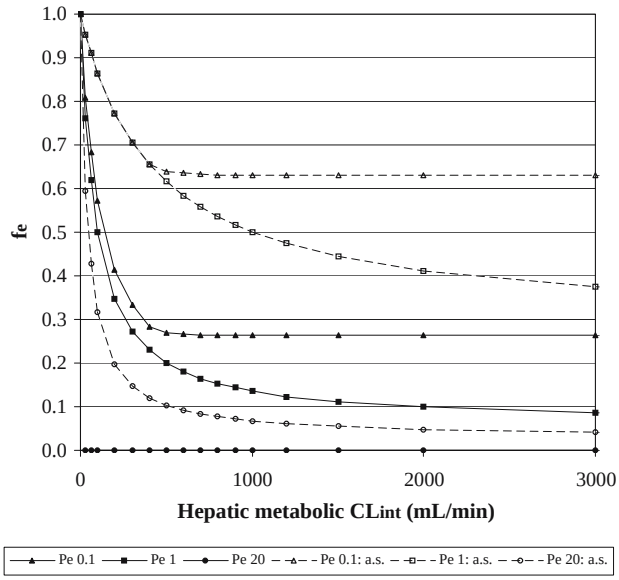

Fig. 11. The predicted relationship between *in vivo* hepatic metabolic CL_{int} and *in vivo* f_e for filtrated (CL_R=125 ml/min) and actively secreted (a.s.; CL_R=600 ml/min) compounds with different levels of passive P_e (0.1×10^{-6} cm/s; Class IV, 1×10^{-6} cm/s; Class III and 20×10^{-6} cm/s; Class I) in humans.

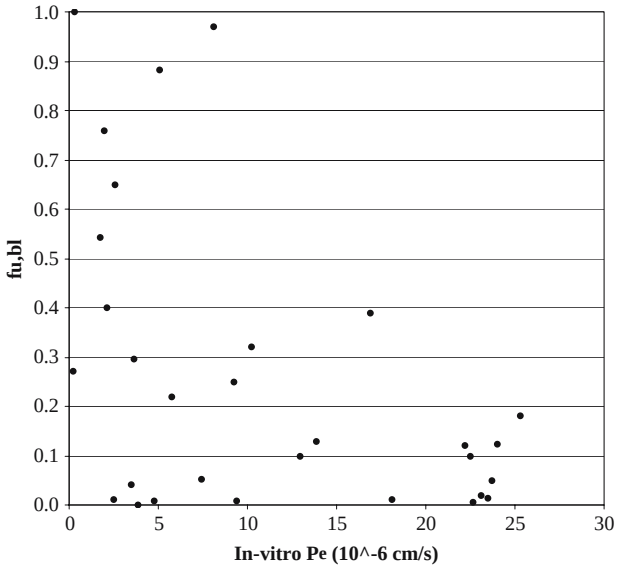

Fig. 12. The relationship between *in vitro* artificial membrane P_e and $f_{u,bl}$ in humans (n=30).

P_e=1.2×10^{-6} cm/s) and acetylsalicylic acid ($E_{u,H}$=0.85; P_e=1.9×10^{-6} cm/s) are compounds with apparent P_e-limited hepatic uptake and can serve as reference compounds. The similarity between the $f_{a,H}$ in three animal species and human $E_{u,H}$ of acetylsalicylic acid (0.6–0.8 in animals *vs* 0.85 in man) further indicates species similarities in hepatic uptake capacity, and gives some validity to the predicted P_e *vs* $f_{a,H}$-curve and P_{e50} and λ-estimates. The slightly higher human estimate might be due to the comparably low Q_H (the Q_H is ~2/3 lower than predicted by allometry) and long hepatic TT in humans (40).

Bile Excretion Potential

Compounds absorbed into hepatocytes might undergo excretion into bile and the upper intestine, and then wholly or partly, be reabsorbed by the intestines (and maybe also from the bile duct). The rate-limiting step for excretion of unbound drug into bile could be either transport across the sinusoidal membrane (on the blood side of hepatocytes) or the canalicular membrane (on the biliary side of hepatocytes). Low extent of biliary excretion is expected for substances with low hepatocyte P_e, high metabolic CL_{int} and high P_e (complete intestinal reabsorption). Active transport across the canalicular membrane and comparably low transport capacity (low P_e) back to blood are probably required for significant bile excretion to occur. Passive transport from the inside of hepatocytes back to blood is favoured by the higher S and P_e of the sinusoidal membrane, and sink conditions (provided by a high Q_H and binding to blood components), whereas passive transport in the bile direction is limited by the smaller S and lower passive P_e of the canalicular membrane, slow bile flow rate (less than a per cent of the Q_H) and potentially high drug concentration in bile (16,41,42).

The potential requirement for active transport, the role of metabolism, and the similarity between biliary and intestinal transporters [efflux proteins in the canalicular

membrane, such as MRP2, P-gp (MDR1) and BCRP, also exist as efflux proteins in the human intestine (43)] make bile excretion difficult to predict.

The predicted/simulated P_e *vs* $E_{max,bile}$-relationships are demonstrated in Fig. 4. These simulations show that the highest bile excretion potential for a compound with no active transport and no passive efflux is expected for substances with a P_e between ~0.1 and ~2.5×10^{-6} cm/s (P_e>P_e of enalaprilat and <P_e of acetaminophen, cimetidine, caffeine and prednisolone; intermediate P_e). A maximum $E_{max,bile}$ of 0.5 is shown for compounds with a P_e of approximately 0.8×10^{-6} cm/s, which corresponds to a P_e of that for amiloride, digoxin, enoxacin, and tetracycline. Because of the anticipated involvement of active bile excretion and intestinal efflux this prediction is probably irrelevant. Different profiles for compounds with complete uptake into bile and passive intestinal reabsorption (with and without 5-fold efflux ratio) are demonstrated (Fig. 4).

Compounds with moderate to high P_e and f_a are expected to show most pronounced EHC plasma concentration *vs* time-profiles (with additional peaks following gallbladder emptying and reabsorption). The typical EHC plasma concentration *vs* time-profile has been demonstrated for many low CL_{int}-compounds with efflux (P-gp) and moderate to high P_e and f_a. Examples include amlodipine, warfarin, digoxin, morphine and indomethacin (43–45).

Oral Bioavailability Potential

The relationships between P_e and F_{min} are shown in Figs. 5 and 10. Compounds with a passive P_e between approximately 0.25 and 2.5×10^{-6} cm/s are anticipated to have a F_{min} of at least ~0.05–0.1. A maximum F_{min} of ~0.2 is obtained at a P_e of approximately 0.8×10^{-6} cm/s, which is similar to that of amiloride, atenolol, digoxin, enoxacin and tetracycline. The results with this simple P_e-based approach can be used alone (without metabolism data) for approximating the potential suitability of candidate drugs for oral administration.

Figure 5 demonstrates the relationships between P_e and observed F and $f_{a,I}$ and predicted F_{min} and $f_{a,I}$. It is anticipated that F values lie between the predicted lines for F_{min} and $f_{a,I}$, and this seems to hold quite well.

Lower F_{min}-values are expected for compounds with active intestinal efflux, active hepatic uptake, dissolution limitations, and significant first-pass gut-wall extraction (especially for high CL_{int}-substrates for CYP3A4 and conjugating enzymes).

The main obstacle for oral F of soluble compounds with a P_e corresponding to <0.4 $f_{a,I}$ (>60% unabsorbed drug and <60% $f_{a,H}$) appears to be intestinal absorption rather than hepatic extraction (regardless of the metabolic capacity of the liver).

Renal Tubular Reabsorption

Figures 6 and 7 show the relationship between passive *in vitro* P_e and *in vivo* $f_{ra,R}$. Despite the variability and uncertainty it was possible to establish reasonable fits to these data. The P_{e50} and λ for the data set containing compounds with apparently negligible active secretion are approximated to 1.4×10^{-6} cm/s and 3.3, respectively (Table I). A similar relationship (upper P_e-limit *vs* $f_{ra,R}$), shifted a magnitude to the right, was found for actively secreted compounds with high passive P_e (Fig. 7). The estimated P_{e50} and λ for this relationship are 12×10^{-6} cm/s and 5, respectively (Table I).

Figures 8 and 9 show the relationships between passive P_e and CL_R (n=20) and passive P_e and f_e (n=23), respectively. They further demonstrate the decreased $f_{ra,R}$ with increasing passive P_e and the importance of active secretion. In addition, they demonstrate the difficulty to predict CL_R when active renal processes are involved. It appears virtually impossible to predict the CL_R for actively secreted substances with a passive P_e<15×10^{-6} cm/s without having *in vitro* $CL_{int,secr}$-data and an established relationship between *in vitro* and *in vivo* $CL_{int,secr}$.

Based on these data it is expected that compounds with a P_e<1×10^{-6} cm/s (P_e<P_e of amiloride, bumetanide, and tranexamic acid) have low tubular reabsorption potential and a P_e>20×10^{-6} cm/s (P_e>P_e of alprenolol, carbamazepine, diclofenac, nifedipine and phenytoin) have high tubular reabsorption potential regardless of the efficiency of secretion transporters.

The $f_{ra,R}$ is determined by the brush-border P_e (passive and active) and S, and intralumenal radius, flow characteristics and residence time (16,46). Regional differences of these determinants exist, but they are not well characterized and understood. There is apparently no TT-estimate available for passage through the human renal tubuli. The net diffusion of weak acids and bases could be influenced by the pH-gradient that exists between tubular fluid (pH=6.3–7.4; average urine pH=6.3) and blood (average pH=7.4) (16).

Renal tubular cells have comparably low passive P_e, and the basolateral membrane (on the blood side) has lower passive P_e than the brush-border membrane on the lumenal side (47). Madin–Darby canine kidney (MDCK) cells have a passive P_e similar to that of the intestinal Caco-2 cell line (which has a comparably low passive tubular excretion capacity) (1,17,48). The proximal tubuli is the primary site of carrier-mediated transport from blood to tubular fluid and urine (46,47). A remarkable heterogeneity in secretion capacity exists along the proximal tubuli (47), and this is one of the factors that make predictions of renal drug elimination of actively secreted compounds difficult. The basolateral and brush-border tubular cell membranes differ with regards to both passive permeation ability sets of transporter proteins (46,47).

Tubular cell uptake from the blood is limited by a short residence time. The ratio of renal blood volume [100 ml (15)] and Q_R gives a TT of ~5 s. According to Rowland and Tozer (49), the TT at the proximal tubular secretory site is ~30 s. The short TT and low passive basolateral P_e indicate low renal excretion capacity by passive diffusion. Despite the short time for uptake into tubular cells some compounds could undergo efficient active renal secretion (16).

Brain Uptake

The BBB is generally looked upon as having low P_e, and being impermeable to drug molecules above or below certain

MW, lipohilicity (log D) and polar surface area (PSA) limits. It has been suggested that in order to penetrate the BBB the PSA, log D and MW should be kept <70–120 Å^2 (depending on source), at 1–4, and <~450 g/mole (50–53). CNS uptake at the comparably permeable choroid plexus is limited by the small S (~1/5,000 of the S_B) (54,55). The weight, Q and TT of the human brain (for a 70 kg's person) are reported to be ~1,500 g (average from 7 reports), 610 ml/min (average from 18 reports) and ~5 s, respectively (14,15). The human brain is comparably large (2.2, 0.75 and 0.39% of body weight in humans, rats and rabbits, respectively) (56), and has a longer TT and greater S than smaller species.

Since the P_e is a rate, all compounds with a P_e will be able to cross the BBB. Low BBB P_e and high extent of brain binding imply that it takes longer time to reach equilibrium between brain tissue and blood (57). There are, not surprisingly, compounds with PSA and MW above the suggested limits with CNS uptake and activity, and MW- or PSA-thresholds for CNS uptake have not yet been established. Lundquist et al. (17), van de Waterbeemd *et al*. (50), Syvänen *et al*. (57), van Asperen *et al*. (58), Clark (59), Tamai and Tsuji (60) and Berezowski *et al*. (61) show CNS-penetrating compounds (in rats and mice in vivo and bovine BBB in vitro) with PSA between 136 and 279 Å^2. Octa- and heptapeptides with MW>1,000 g/mol enter the CNS in rats and mice (55,62). Inulin (MW ~5,000 g/mol) is also taken up by the rat BBB (63), and it has a lower BBB P_e than other studied low P_e molecules, including sucrose (often used as a reference substance), vincristin and cyclosporin (61,64).

The BBB has a cholesterol/phospholipid ratio (0.7) similar to that of other endothelial cells (65), and its thickness is comparably thin (0.3–0.5 μm *vs* 17–30 μm or enterocytes) (66, 67). Compared to the intestinal Caco-2 cells the *in vitro* P_e of BBB cells (bovine brain endothelia cells co-cultured with primary rat astrocytes) for 15 substances were on average 11-fold more permeable (maximally 34-fold more permeable) (17). This suggests that BBB permeation is no limitation for the CNS uptake of intestinally absorbed compounds without efficient BBB efflux. Rapid on-set of CNS-effects (seconds) for many drugs (including anaesthetics and nicotine) verifies the high uptake capacity of the brain. Compounds with brain $P_eS>Q_B$ have been found in the rat (68). Brain uptake index (BUI; fraction absorbed by the brain during a short brain perfusion)-data obtained in the rat also demonstrate rapid and extensive *in vivo* brain uptake of high P_e compounds and some absorption of low P_e-substances. For example, antipyrine, caffeine, nicotine and propranolol were absorbed to ~70–100% within 5–15 s, and the uptake of hydrocortisone and sucrose was 1.4% (17).

Active transport across the BBB can also occur. There are transport proteins for efficient influx (transporters for glucose, amino acids and small peptides) and efflux [such as P-gp on the luminal (blood) side and OAT3 on the abluminal (brain tissue) side] in the BBB (54,57,69).

Lennernäs (69) demonstrated a quite good correlation between animal BBB log P_e-estimates and human small intestinal in vivo log P_e (n=11; actively transported compounds inclusively), and Lundquist *et al*. (17) showed that log P_eS- and BUI (5–15 s after injection)-data obtained in the rat correlated well with log *in vitro* BBB P_e (r=0.93–0.95; n=13). This validates the *in vitro* BBB P_e-method for predictions of *in vivo* BBB P_e in the rat. Artifical membrane P_e appears, however, a rather poor predictor of *in vitro* BBB P_e (r=0.43). Among possible reasons are active transport *in vivo* and differences in membrane/barrier characteristics between these models.

Figure 10 shows the estimated relationship between artifical membrane *in vitro* P_e and human *in vivo* $f_{a,B}$. It should be noted that this is a rough approximation. The $f_a = P_{e50}^{\lambda} / \left(P_{e50}^{\lambda} + P_e^{\lambda}\right)$ -approach was used to model the relationship, but the result was not satisfactory. The P_e *vs* f_a-relationship is different from those for other organs (with a shallow λ up to a certain P_e-level and steep λ at P_e above that limit). A better fit was obtained when using separate estimates for compounds with low (<10×10^{-6} cm/s) and high P_e (>10×10^{-6} cm/s; corresponding to a P_e of that of betaxolol, dexamethazone, flunitrazepam and prednisolone). Hansen *et al*. (70) also found a similar relationship between log *in vitro* BBB P_e and *in vivo* brain uptake CL in the rat (assessed by microdialysis sampling). The P_{e50} and λ for the low and high P_e-compounds are estimated to 150 and 24×10^{-6} cm/s, and 0.7 and 2, respectively (Table I). Predicted estimates for humans agree quite well with BUI-data obtained in the rat (see above).

Due to the short brain TT it is not anticipated that unbound drug molecules are completely absorbed during one passage through the human brain. High P_e substances will be located at the steepest part of the P_e *vs* $f_{a,B}$-curve, which makes their brain uptake potentially more sensitive to involvement and changes of active transport than in the other studied organs.

The Permeability-Based Classification System (PCS)

The P_e *vs* f_a- and f_{ra}-relationships in the different organs/tissues were the basis for the development of a P_e-based PK classification system (PCS) with four classes (I–IV; Fig. 10, Table II). Depending on the involvement and magnitude of active transport a compound could belong to different *in vitro* and *in vivo* PCS Classes. The intention is that the organ uptake, elimination routes, and active transport, drug–drug interaction and drug and metabolite organ accumulation/toxicity potentials can be approximated with this system. The overall P_e (passive or passive+active) of compounds in early drug discovery can be modified in order to improve PK characteristics, and change main elimination route(s) and tissue accumulation potential. The PCS should be used together with hepatic metabolic CL_{int} (preferably obtained with human hepatocytes), $f_{u,bl}$ and active transport data. Steep slopes, similar P_{e50} for some organs, and variability/uncertainty show a potential for incorrect classification and the requirement for high quality P_e-data. Shapes, shifts and qualities of the predicted curves could possibly be different with other P_e-models. Other P_e-models could include active transport processes, and it is also possible to have separate P_e-model for the organs (e.g. intestinal, BBB, hepatic and renal cell lines). PCSs for animals could also be easily established based upon available animal *in vivo* f_a-data.

The role of P_e for the f_e of compounds with different hepatic metabolic *in vivo* CL_{int} is demonstrated in Fig. 11. The P_e in these simulations was set to 0.1 (Class IV), 1 (Class III) and 10 (Class II)$\times10^{-6}$ cm/s, the f_u was set to 1, and the

CL_R was set to GFR (125 ml/min; filtration only) or 600 ml/min (filtration+efficient active secretion). Class I compounds are expected to have zero or negligible f_e. Compounds with very low P_e (Class IV) are anticipated to be excreted renally to some extent, especially if the metabolic CL_{int} is low.

The liver and brain have highly permeable endothelia, whereas the intestinal and renal tubular epithelia have low uptake capacity. For an unbound compound with a P_e of 1×10^{-6} cm/s (similar to the passive *in vitro* P_e of digoxin, enoxacin and tetracyclin) the hepatic, brain, intestinal and renal tubular f_a are approximately 75, 3, 66 and 25%, respectively. The average % f_a per second in the liver, brain and intestines are approximately 2.4, 0.6 and 0.002%, respectively. Corresponding average % f_a per minute per absorptive S (m^2) are 0.8, 1.8 and 0.002, respectively. These estimates were based on 31, 5 s and 8.4 h TT, and 180, 20 and 70 m^2 S, respectively.

Figure 12 shows a rather poor relationship between P_e and $f_{u,bl}$ (r^2=0.22; n=30), but that high P_e-compounds are less likely to demonstrate high $f_{u,bl}$-values than low P_e-substances. Maximum $f_{u,bl}$-values for low ($<8\times10^{-6}$ cm/s), moderate and high ($>20\times10^{-6}$ cm/s) P_e-substances in this data set are ~1.0, ~0.4 and ~0.2, respectively. Many Class III and IV compounds have comparably high $f_{u,bl}$-values, which indicates that they have potential for high CL_R. The trend that many low P_e-substances have lower binding capacity to blood components could possibly be explained by a higher degree of hydrophilicity of these compounds. The association rate to blood components could be of importance for the ADME/PK, especially for compounds that bind extensively. Compounds that bind slowly to red blood cells have also been shown to have low lipophilicity and P_e (71,72), which indicates that their (a generalization) extent of equilibrium binding probably is not very extensive.

According to the BDDCS, compounds with a $P_e\geq2.5\times10^{-6}$ cm/s and $f_{a,I}\geq0.9$ are classified as highly permeable and are expected to be eliminated mainly by hepatic metabolism. Figure 10 shows that the P_e-limit of BDDCS is too low (~8-fold; 2.5 *vs* 20×10^{-6} cm/s). Compounds with a P_e between 2.5 and 20×10^{-6} cm/s (especially those with low metabolic CL_{int}) could be significantly and mainly eliminated via urine and/or bile. This is clearly demonstrated in Fig. 1. Many low P_e-compounds (based on the BDDCS P_e-limit) have comparably high extent and degree of metabolism, and there are several high P_e-drugs with minor metabolism. Advantages of the PCS compared to the BDDCS include a higher and more balanced P_e-limit for metabolism as major elimination route, a continuous P_e-scale, consideration of P_e *vs* f_a-relationships (including useful equations) of various important organs, four instead of two P_e-classes, and the possibility to apply it for prediction and evaluation of potential drug–drug transporter interactions and for organ/cell trapping of drugs and their metabolites.

Shortcomings with the PCS include the uncertainty of derived *in vivo* f_a- and f_{ra}-data, limited amount of *in vivo* data for hepatic uptake, the requirement to include rat liver and brain uptake data, potential P_e-differences between the *in vitro* method (*in vitro* P_e was calculated from membrane affinities) and in vivo, and potential risk for incorrect classification of compounds (especially those with significant active transport and those who have a P_e close to an adjacent class).

The PCS is also applicable for animals. The shapes, shifts and placings of P_e *vs* f_a-relationships in rat intestines, liver and brain appear to be similar to those in humans (Fagerholm, unpublished data).

Drug–Drug Transport Interactions

Equation 1 and the established P_{e50}- and λ-estimates can be used to simulate the effects of changed P_e (such as involvement and changes of active transport) on the uptake of the studies organs.

The intestinal, liver and brain absorption of compounds with a P_e at or near the steepest part of the P_e *vs in vivo* f_a-relationships is potentially more sensitive to changes of active P_e, such as a result of saturation, inhibition or induction. The establishment of these P_e *vs* f_a-relationships could therefore be of great value for predicting drug–drug interactions on a transporter level in many important organs. The shift of the curves may also indicate in which organ(s) the interaction potential is anticipated to be greatest. For example, it is less likely to find clinically significant drug–drug *efflux* interactions for Class I compounds in the intestines, than it is in the brain.

The impact of changes in passive and/or active P_e on the uptake in the studied organs could easily be demonstrated with curves presented in Fig. 10. For example, for a compound with a passive P_e of 20×10^{-6} cm/s (Class I) in this system a 4-fold active efflux (reducing the overall P_e to 5×10^{-6} cm/s; Class II) would lead to virtually unchanged intestinal and hepatic uptake, but 4-fold decreased brain uptake.

The $f_{a,I}$ of the highly permeable compound and P-gp substrate verapamil in humans *in vivo* is unaffected by dose (the efflux is more pronounced and overall P_e is lower at lower intestinal concentrations) (73), but its brain uptake in vivo in rats during infusion is significantly enhanced in the presence of the P-gp inhibiting cyclosporin (57). Animal in vivo studies have demonstrated significantly enhanced brain/plasma-ratios for highly permeable substances in animals lacking P-pg (58,74). The P-gp inhibitor quinidine was able to increase the brain uptake of the highly (passive) permeable P-pg substrate loperamide in humans, and thereby, causing respiratory depression (75). These changes could not be explained by increased plasma exposure to loperamide. Drug-drug transport interactions in the intestines and liver/bile have been found for several low passive P_e-compounds. These include those observed for digoxin (intestinal), fexofenadine (intestinal) and pravastatin (liver/bile) (76–79).

Drug and Metabolite Organ Accumulation, *Trapping* and Toxicity

The P_e could potentially also play a role in organ accumulation, *trapping* and toxicity of drugs and metabolites. For example, compounds with good metabolic stability and given at high doses could concentrate in the renal tubular fluid and urine (if low passive P_e, with or without active secretion) or be efficiently absorbed by the upper renal tubular mucosa (if high passive P_e), and thereby, cause local mucosal damage. The potential for upper GI mucosal damage is generally

greatest for highly permeable and soluble drugs given at high oral doses (acids in particular; such as non-steroidal anti-inflammatory drugs). The PCS could therefore be useful when predicting compounds expected to accumulate in metabolizing cells and the renal tubuli.

Lipophilic basic compounds generally bind extensively to cell components, especially to mitochondria and lysosomes (the liver, lungs and kidneys belong to the lysosyme-rich organs) (80). Compounds with low passive P_e, efficient influx and low metabolic CL_{int} also have a comparably high intracellular accumulation capacity.

The P_e of a drug and the P_e-ratio between drug and metabolite(s) are important for hepatocyte metabolite accumulation potential. A significant intracellular accumulation may occur for low P_e-metabolites of high P_e-compounds with high CL_{int}.

Local and systemic exposures could be poorly correlated for compounds with metabolite-related liver toxicity and drug-induced renal tubular damage. On this basis, it is questionable whether systemic exposures of such compounds and metabolites could be used to set appropriate safety limits.

CONCLUSION

The role of P_e in drug ADME/PK, interactions and toxicity was evaluated using a literature data set of *in vitro* artificial membrane P_e, and estimates of *in vivo* f_a in the human intestines, liver, kidneys (reabsorption) and brain (predicted). In comparison, the liver and brain have very high passive uptake capacity and short passage time for absorption. Due to these differences there are shifts and different shapes of P_e *vs* f_a-curves. Based on these relationships, including predicted curves for bile excretion potential and F_{min}, a P_e-based ADME/PK Classification System (PCS) was developed. Class I compounds (very high P_e) are expected to be eliminated mainly by metabolism. Compounds of Classes II (high P_e) and III (intermediate P_e and incomplete f_a) have highest F_{min} potential. Class III and IV compounds (low/moderate passive P_e and f_a) have lowest metabolism and highest excretion potentials (especially when active renal secretion and bile efflux are involved).

Potential safety risk related drug–drug transport interactions (increased exposure) in the intestines (inhibited efflux), liver (inhibited influx) and brain (inhibited efflux) are most likely to occur for compounds at and close to the P_e *vs* f_a-slopes and with significant active transport. That implies that such interactions are most likely to occur for high passive P_e-compounds in the brain, and low passive P_e-compounds in the intestines and liver/bile.

The potential for accumulation in tubular fluid is greatest for substances with good metabolic stability, low passive P_e and efficient active secretion. Low P_e-metabolites of high P_e-compounds have higher potential to accumulate in metabolizing cells.

The PCS and high quality P_e-data (with and without active transport), as a complement to traditional metabolic CL_{int}- and $f_{u,bl}$-measurements, are believed to be useful for predictions of ADME/PK and elimination routes, and potential interactions and organ accumulation, *trapping* and toxicity in humans. It has several advantages compared to the previously developed BDDCS.

ACKNOWLEDGMENTS

The author greatly acknowledges Professor Per Artursson at Uppsala University, Sweden, Associate Professor Anna-Lena Ungell at AstraZeneca R&D Mölndal, Sweden, and Doctors Lovisa Afzelius and Janet Hoogstraate at AstraZeneca R&D Södertälje, Sweden, for reviewing the manuscript, for valuable comments and advise, and for support.

REFERENCES

1. U. Fagerholm, D. Nilsson, L. Knutson, and H. Lennernäs. Jejunal permeability in humans *in vivo* and rats *in situ*: investigation of molecular size selectivity and solvent drag. *Acta Physiol. Scand.* **165**:315–324 (1999).
2. U. Fagerholm. In Characteristics of intestinal permeability in humans *in vivo* and rats *in situ*. Doctoral thesis, Uppsala University, Sweden (1997).
3. U. Fagerholm, and H. Lennernäs. Experimental estimation of the effective unstirred water layer thickness in the human jejunum, and its importance in oral drug absorption. *Eur. J. Pharm. Sci.* **3**:247–253 (1995).
4. Y. Shibata, H. Takahashi, M. Chiba, and Y. Ishii. Prediction of hepatic clearance and availability by cryopreserved human hepatocytes: an application of serum incubation method. *Drug Met. Disp.* **30**:892–896 (2002).
5. C.-Y. Wu, and L. Benet. Predicting drug disposition via application of BCS: Transport/absorption/elimination interplay and development of a biopharmaceutics drug disposition classification system. *Pharm. Res.* **22**:11–23 (2005).
6. U. Fagerholm. Evaluation and suggested improvements of the Biopharmaceutics Classification System (BCS). *J. Pharm. Pharmacol.* **59**:751–757 (2007).
7. S. Willmann, W. Schmitt, J. Keldenich, J. Lippert, and J. B. Dressman. A physiological model for the estimation of the fraction dose absorbed in humans. *J. Med. Chem.* **47**:4022–4031 (2004).
8. A. Goodman Gilman. In J. G. Hardman, L. E. Limbird, and A. Goodman Gilman (eds.) The pharmacological basis of therapeutics. McGraw-Hill (2001).
9. R. S. Obach. Prediction of human clearance of twenty-nine drugs from hepatic microsomal intrinsic clearance data: an examination of *in vitro* half-life approach and nonspecific binding to microsomes. *Drug Met. Disp.* **27**:1350–1359 (1999).
10. R. J. Riley, D. F. McGinnity, and R. P. Austin. A unified model for predicting human hepatic, metabolic clearance from *in vitro* intrinsic clearance data in hepatocytes and microsomes. *Drug Met. Disp.* **33**:1304–1311 (2005).
11. U. Fagerholm, M. Johansson, and H. Lennernäs. Comparison between permeability coefficients in rat and human jejunum. *Pharm. Res.* **13**:1336–1342 (1996).
12. W. L. Chiou, and P. W. Beuhler. Comparison of oral absorption and bioavailability of drugs between monkey and human. *Pharm. Res.* **19**:868–874 (2002).
13. J. Mordenti. Man *vs* beast: pharmacokinetic scaling in mammals. *J. Pharm. Sci.* **75**:1028–1040 (1986).
14. S. L. Lindstedt, and P. J. Schaeffer. Use of allometry in predicting anatomical and physiological parameters of mammals. *Lab. Animals.* **36**:1–19 (2002).
15. R. W. Leggett, and L. R. Williams. A proposed blood circulation model for reference man. *Health Physics.* **69**:187–201 (1995).
16. M. Rowland, and T. N. Tozer. In Clinical pharmacokinetics: concepts and applications. M. Rowland and T.N. Tozer (eds.). Williams and Wilkins (1995).
17. S. Lundquist, M. Renftel, J. Brillault, L. Fenart, R. Cecchelli, and M.-P. Dehouck. Prediction of drug transport through the blood–brain barrier *in vivo*: a comparison between *in vitro* cell models. *Pharm. Res.* **19**:976–981 (2002).

18. J. T. Goodwin, and D. E. Clark. In silico predictions of blood–brain barrier penetration: Considerations to "keep in mind". *J. Pharmacol. Exp. Ther.* **315**:477–483 (2005).
19. Y. Sawada, M. Hanano, Y. Sugiyama, H. Harashima, and T. Iga. Prediction of the volumes of distribution of basic drugs in humans based on data from animals. *J. Pharmacokin. Biopharm.* **12**:587–596 (1984).
20. Y. Sawada, M. Hanano, Y. Sugiyama, and T. Iga. Prediction of the disposition of nine weakly acidic and six weakly basic drugs in humans from pharmacokinetic parameters in rats. *J. Pharmacokin. Biopharm.* **13**:477–492 (1985).
21. P. Poulin, and F.-P. Theil. Prediction of pharmacokinetics prior to *in vivo* studies. 1. Mechanism-based prediction of volume of distribution. *J. Pharm. Sci.* **91**:129–156 (2002).
22. U. Fagerholm, and M. A. Björnsson. Clinical pharmacokinetics of the cyclooxygenase-inhibiting nitric oxide donating donator (CINOD) AZD3582. *J. Pharm. Pharmacol.* **57**:1539–1554 (2005).
23. J. B. Dressmann, G. L. Amidon, C. Reppas, and V. P. Shah. Dissolution testing as a prognostic tool for oral drug absorption: immediate release dosage forms. *Pharm. Res.* **15**:11–22 (1998).
24. D. Hörter, and J. B. Dressmann. Influence of physicochemical properties on dissolution of drugs in the gastrointestinal tract. *Adv. Drug Del. Rev.* **46**:75–87 (2001).
25. A. Lindahl, A.-L. Ungell, L. Knutson, and H. Lennernäs. Characterization of fluids from the stomach and proximal jejunum in men and women. *Pharm. Res.* **14**:497–502 (1997).
26. B. Abrahamsson. In Biopharmaceutical aspects of extended release tablets based on the hydrophilic matrix principle. Doctoral thesis, Uppsala University, Sweden (1997).
27. M. F. Paine, D. D. Shen, K. L. Kunze, J. D. Perkins, C. L. Marsh, J. P. McVicar, D. M. Barr, B. S. Gillies, and K. E. Thummel. First-pass metabolism of midazolam by the human small intestine. *Clin. Pharmacol. Ther.* **60**:14–24 (1996).
28. T. Mizuma, K. Kawashima, S. Sakai, S. Sakaguchi, and M. Hayashi. Differentiation of organ availability by sequential and simultaneous analyses: intestinal conjugative metabolism impacts on intestinal availability in humans. *J. Pharm. Sci.* **94**:571–575 (2005).
29. L. Borgström, L. Nyberg, S. Jonsson, C. Lindberg, and J. Paulson. Pharmacokinetic evaluation in man of terbutaline given as separate enantiomers and as the racemate. *Br. J. Clin. Pharmacol.* **27**:49–56 (1989).
30. I. De Waziers, P. H. Cugnenc, C. S. Yang, J. P. Leroux, and P. H. Beaune. Cytochrome P450 isoenzymes, epoxide hydrolase and glutathione transferases in rat and human hepatic and extrahepatic tissues. *J. Pharmacol. Exp. Ther.* **253**:387–394 (1990).
31. X. Cao, S. T. Gibbs, L. Fang, H. A. Miller, C. P. Landowski, H.-C.Shin, H. Lennernäs, Y. Zhong, G. L. Amidon, L. X. Yu, and D. Sun. Why is it challenging to predict intestinal drug absorption and oral bioavailability in human using rat model? *Pharm. Res.* **23**:1675–1686 (2006).
32. E. G. van de Kerkhof, A.-L. B. Ungell, Å. K. Sjöberg, M. H. Jager, C. Hilgendorf, I. A. M. de Graaf, and G. M. M. Groothuis. Innovative methods to study human intestinal drug metabolism *in vitro*: precision-cut slices compared with Ussing chamber preparations. *Drug Met. Disp*. **34**:1893–1902 (2006).
33. U. Fagerholm, A. Lindahl, and H. Lennernäs. Regional intestinal permeability in rats of compounds with different physicochemical properties and transport mechanisms. *J. Pharm. Pharmacol.* **49**:687–690 (1997).
34. S. S. Davis. Evaluation of the gastrointestinal transit of pharmaceutical dosage forms using the technique of gammascintigraphy. *S.T.P Pharma.* **2**:1015–1022 (1986).
35. G. Alpini, R. A. Garrick, M. J. T. Jones, R. Nunes, and N. Tavoloni. Water and nonelectrolyte permeability of isolated rat hepatocytes. *Am. J. Physiol.* **251**:C872–882 (1986).
36. A. Blouin. Morphometry of liver sinusoidal cells. In E. Wisse, Knook, D. L. (eds.) Kupffer Cells and Other Liver Sinusoidal Cells (1977).
37. C. A. Goresky, K. S. Pang, A. J. Schwab, F. Barker III, W. F. Cherry, and G. G. Bach. Uptake of a protein-bound polar compound, acetaminophen sulphate, by perfused rat liver. *Hepatol.* **16**:173–190 (1992).
38. A. J. Schwab, F. Barker III, C. A. Goresky, and K. S. Pang. Transfer of enalaprilat across rat liver cell membranes is barrier limited. *Am. J. Physiol.* **258**:G461–475 (1990).
39. G. D. Mellick, and M. S. Roberts. The disposition of aspirin and salicylic acid in the isolated perfused rat liver: The effect of normal and retrograde flow on availability and mean transit time. *J. Pharmacy Pharmacol.* **48**:738–743 (1996).
40. H. Boxenbaum. Interspecies variation in liver weight, hepatic blood flow, and antipyrine intrinsic clearance: Extrapolation of data to benzodiazepines and phenytoin. *J. Pharmacokin. Biopharm.* **8**:165–176 (1980).
41. E. R. Weibel, W. Staubli, H. R. Gnagi, and F. A. Hess. Correlated morphometric and biochemical studies on the liver cell. Morphometric model, and normal morphometric data for rat liver. *J. Cell Biol.* **42**:68–91 (1969).
42. P. J. Meier, E. S. Sztul, A. Reuben, and J. L. Boyer. Structural and functional polarity of canalicular and basolateral plasma membrane vesicles isolated in high yield from rat liver. *J. Cell Biol.* **98**:991–1000 (1984).
43. TP-search transport database (http://www.TP-search.jp/). Y. Sugiyama, H. Kusuhara, K. Maeda and Y. Nozaki (accessed 04/11/07).
44. M. S. Roberts, B. M. Magnusson, F. J. Burczynski, and M. Weiss. Enterohepatic circulation. Physiological, pharmacokinetic and clinical implications. *Clin. Pharmacokin.* **41**:751–790 (2002).
45. D. Raušl, N. Fotaki, R. Zanoški, M. Vertzoni, B. Cetina-Èimek, M. Z. I. Khan, and C. Reppas. Intestinal permeability and excretion into bile control the arrival of amlodipine into the systemic circulation after oral administration. *J. Pharm. Pharmacol.* **58**:827–836 (2006).
46. Y. Shitara, H. Sato, and Y. Sugiyama. Evaluation of drug–drug interaction in the hepatobiliary and renal transport of drugs. *Annu. Rev. Pharmacol.Toxicol.* **45**:689–723 (2005).
47. R. Masereeuw, and F. G. M. Russel. Mechanisms and clinical implications of renal drug excretion. *Drug Met. Rev.* **33**:299–351 (2001).
48. J. D. Irvine, L. Takahashi, K. Lackhart, J. Cheong, J. W. Tolan, H. E. Selick, and J. R. Grove. MDCK (Madin–Darby canine kidney) cells: a tool for membrane permeability screening. *J. Pharm. Sci.* **88**:29–33 (1999).
49. M. Rowland, and T. N. Tozer. In Clinical pharmacokinetics: concepts and applications. Lea and Febiger (1989).
50. H. van de Waterbeemd, G. Camenisch, G. Folkers, J. R. Chretien, and O. A. Raevsky. Estimation of blood–brain barrier crossing of drugs using molecular size and shape, and h-bonding descriptors. *J. Drug Targ.* **6**:151–165 (1998).
51. J. Kelder, P. D. J. Grootenhuis, D. M. Bayada, L. P. C. Delbressine, and J.-P. Ploemen. Polar molecular surface as a dominating determinant for oral absorption and brain penetration of drugs. *Pharm. Res.* **16**:1514–1519 (1999).
52. W. M. Pardridge. Blood–brain barrier drug targeting: the future of brain drug development. *Molec. Intervent.* **3**:90–105 (2003).
53. W. P. Pardridge. The blood–brain barrier: bottleneck in brain drug development. *NeuroRx.* **2**:3–14 (2005).
54. D. J. Begley. The blood–brain barrier: principles for targeting peptides and drugs to the central nervous system. *J. Pharm. Pharmacol.* **48**:136–146 (1996).
55. T. J. Abbruscato, S. A. Thomas, V. J. Hruby, and T. P. Davis. Blood–brain barrier permeability and bioavailability of a highly potent and μ-selective opioid receptor antagonist, CTAP: comparison with morphine. *J. Pharmacol. Exp. Ther.* **280**:402–409 (1997).
56. J. Kawakami, K. Yamamoto, Y. Sawada, and T. Iga. Prediction of brain delivery of ofloxacin, a new quinolone, in the human from animal data. *J. Pharmacokin. Biopharm.* **22**:207–227 (1994).
57. S. Syvänen, G. Blomquist, M. Sprycha, A. U. Höglund, M. Roman, O. Eriksson, M. Hammarlund-Udenaes, B. Långström, and M. Bergström. Duration and degree of cyclosporin induced P-glycoprotein inhibition in the rat blood–brain barrier can be studied with PET. *NeuroImage.* **32**:1134–1141 (2006).
58. J. van Asperen, U. Mayer, O. van Tellingen, and J. H. Beijnen. The functional role of P-glycoprotein in the blood–brain barrier. *J. Pharm. Sci.* **86**:881–884 (1997).
59. D. E. Clark. Rapid calculation of polar molecular surface area and its application to the prediction of transport phenomena. 2.

Prediction of blood–brain barrier penetration. *J. Pharm. Sci.* **88**:815–821 (1999).
60. I. Tamai, and A. Tsuji. Transporter-mediated permeation of drugs across the blood–brain barrier. *J. Pharm. Sci.* **11**:1371–1388 (2000).
61. V. Berezowski, C. Landry, S. Lundquist, L. Dehouck, R. Cecchelli, M. P. Dehouck, and L. Fenart. Transport of drug cocktails through an *in vitro* blood–brain barrier: is it a good strategy for increasing the throughput of the discovery pipeline? *Pharm. Res.* **21**:756–760 (2004).
62. S. A. Thomas, T. J. Abbruscato, V. S. Hau, T. J. Gillespie, J. Zsigo, V. J. Hruby, and T. P. Davis. Structure-activity relationships of a series of [D-Ala^2]deltorphin I and II analogues; *in vitro* blood–brain barrier permeability and stability. *J. Pharmacol. Exp. Ther.* **281**:817–825 (1997).
63. A. Kakee, T. Terasaki, and Y. Sugiyama. Brain efflux index as a novel method of analyzing efflux transport at the blood–brain barrier. *J. Pharmacol. Exp. Ther.* **277**:1550–1559 (1996).
64. M.-P. Dehouck, R. Cecchelli, A. R. Green, M. Renftel, and S. Lundquist. *In vitro* blood–brain barrier permeability and cerebral endothelial cell uptake if the neuroprotective nitrone compound NXY-059 in normoxic, hypoxic and ischemic conditions. *Brain Res.* **955**:229–235 (2002).
65. H. Fischer, R. Gottschlich, and A. Seelig. Blood–brain barrier permeation: molecular parameters governing passive diffusion. *J. Membr. Biol.* **165**:201–211 (1998).
66. J. Karlsson, and P. Artursson. A new diffusion chamber system for the determination of drug permeability coefficients across the human intestinal epithelium that are independent on the unstirred water layer. *Biochim. Biophys. Acta.* **1111**:204–210 (1992).
67. Y. Su, and P. J. Sinko. Drug delivery across the blood–brain barrier: why is it difficult? how to measure and improve it? *Expert Opin. Drug Del.* **3**:419–435 (2006).
68. E. Boström, U. S. H. Simonsson, and M. Hammarlund-Udenaes. *In vivo* blood–brain barrier transport of oxycodone in the rat: Indications for active influx and implications for pharmacokinetics/pharmacodynamics. *Drug Met. Disp.* **34**:1624–1631 (2006).
69. H. Lennernäs. Human jejunal effective permeability and its correlation with preclinical drug absorption models. *J. Pharm. Pharmacol.* **49**:627–638 (1997).
70. D. K. Hansen, D. O. Scott, K. W. Otis, and S. M. Lunte. Comparison of *in vitro* BBMEC permeability and *in vivo* CNS uptake by microdialysis sampling. *J. Pharmaceut. Biomed. Anal.* **27**:945–958 (2002).
71. L. S. Schanker, P. A. Nafpliotis, and J. M. Johnson. Passage of organic bases into human red cells. *J. Pharmacol. Ther.* **133**:325–331 (1961).
72. P. Naccache, and R. I. Sha'afi. Patterns of nonelectrolyte permeability in human red blood cell membrane. *J. Gen. Physiol.* **62**:714–736 (1973).
73. R. Sandström, A. Karlsson, L. Knutson, and H. Lennernäs. Jejunal absorption and metabolism of R/S-verapamil in humans. *Pharm. Res.* **15**:856–862 (1998).
74. A. Tsuji, and I. Tamai. Blood–brain barrier function of P-glycoprotein. *Adv. Drug Del. Rev.* **25**:287–298 (1997).
75. A. J. M. Sadeque, C. Wandel, H., He, S. Shah, and A. J. J. Wood. Increased drug delivery to the brain by P-glycoprotein inhibition. *Clin. Pharmacol. Ther.* **68**:231–237 (2000).
76. S. Hirata, S. Izumi, S. T. Furukubo, M. Ota, M. Fujita, T. Yamakawa, I. Hasegawa, H. Ohtani, and Y. Sawada. *Int. J. Clin. Pharmacol. Ther.* **43**:30–36 (2005).
77. J. Rengelshausen, C. Goggelmann, J. Burhenne, K. D. Reidel, J. Ludwig, J. Weiss, G. Mikus, I. Walter-Sack, and W. E. Haefeli. Contribution of increased oral bioavailability and reduced nonglomerular renal clearance of digoxin to the digoxin–clarithromycin interaction. *Br. J. Clin. Pharmacol.* **56**: 32–38 (2003).
78. R. H. Ho, and R. B. Kim. Transporters and drug therapy: implications for drug disposition and disease. *Clin. Pharmacol. Ther.* **78**:260–277 (2005).
79. FASS web-site http://www.fass.se.
80. G. A. Siebert, D. Y. Hung, P. Chang, and M. S. Roberts. Ion-trapping, microsomal binding, and unbound drug distribution in the hepatic retention of basic drugs. *J. Pharmacol. Exp. Ther.* **308**:228–235 (2004).
81. U. Fagerholm, M. Johansson, and H. Lennernäs. Comparison between permeability coefficients in rat and human jejunum. *Pharm. Res.* **13**:1336–1342 (1996).
82. U. Fagerholm. Prediction of human pharmacokinetics-Gastrointestinal absorption. *J. Pharm. Pharmacol.* **59**:905–916 (2007).